MINISTRY OF EDUCATION

TECHNICAL UNIVERSITY
OF CLUJ-NAPOCA, ROMANIA

Faculty of Electrical Engineering

PhD THESIS
– ABSTRACT –

High-Frequency Modelling of Rotating Electrical Machines

PhD Student:
José Enrique Ruiz-Sarrió

PhD Supervisor:
Prof. Eng. Claudia Steluţa Marţiş

Examination committee:
Chair: Prof. Eng. **Teodor Pană**, PhD – Technical University of Cluj-Napoca, Romania
PhD Supervisor: Prof. Eng. **Claudia Steluţa Marţiş**, PhD – Technical University of Cluj-Napoca, Romania
Members:
Prof. Eng**. Jose A. Antonino-Daviu**, PhD – Universitat Politècnica de València, Spain
Prof. Eng. **Elena Lomonova**, PhD – Eindhoven University of Technology, The Netherlands
Prof. Eng. **Lorand Szabo**, PhD – Technical University of Cluj-Napoca, Romania

– Cluj-Napoca –
2022

TABLE OF CONTENTS

The usage of variable frequency drives for rotating electrical machine operation is a standard technique for supply and control. However, high switching frequencies and voltage gradients *(dv/dt)* can cause problems such as undesired Electromagnetic Interference (EMI), leakage and bearing currents, and machine terminal over-voltages. With the appearance of wide band-gap semiconductors high-frequency phenomena are attracting increased research attention. Following this technology trend, the assessment of the high-frequency response throughout the drive design process becomes of capital importance.

The objective of the present dissertation is to study the high-frequency response of rotating electrical machines. The study of the physical phenomenom is initially tackled by performing a comprehensive analysis of different modelling methodologies and trends. The main core of the thesis focusses on developing and validating a deterministic modelling method that provides an estimation of the machine impedances in a high-frequency band (i.e., from tenths of kHz to thenths of MHz depending on the objective). This prediction is aimed to favor an EMI-awared design of the rotating machine at early stages when a physical prototype is not yet available.

The developed modelling method is implemented and validated for two different PMSMs utilized in the automotive industry. These two machines are selected taking into account the INTERACT project boundaries and partners.

The work presented in this dissertation gave rise to some original contributions shared in peer reviewed international conferences and journals. These research documents are already published or in process of publication. Further information about published material is provided in the section 'List of publications' of the main core of the thesis. The most important contributions developed in this dissertation are:

- The development and validation of a high-frequency impedance model oriented towards early prediction for PMSMs

- The detailed experimental investigation of the effect of PMSM rotor and housing on the high-frequency impedance response

- The detailed experimental investigation of the rotor DC field effect on the high-frequency impedance response in PMSMs

- A thorough numerical investigation of the effect of the machine configuration, geometry and material characteristics on the high-frequency impedance response.

The rotating electrical machine model plays a key role in the full drive simulation. These models represent the machine impedance in different propagation modes over a broad frequency range, usually starting from tenths of kHz until the MHz range. The two main trends for motor modelling are the data-based models obtained from measured impedance curves and the pure numerical models using geometry, material characteristics and machine configuration parameters. The main types of test-based models are the behavioural or black-box models and the physics-based circuits. In the first type, fitting, and synthesis techniques such as vector fitting are utilized to map the measured impedance of the machine. Physics-based circuits attempt to describe the real high-frequency behaviour of the machine by using passive circuit elements. The resonant frequencies of the measured impedances are used to

compute the values of the different passive elements in the circuit. Test-based models need a real machine and measurement equipment to obtain the impedance of the different propagation modes. For this reason, it is not a valid methodology for early-stage design when these resources are not yet available.

The main core of the thesis focusses on developing and validating a deterministic modelling method that provides an estimation of the machine impedances in a high-frequency band (i.e., from tenths of kHz to tenths of MHz). This prediction is aimed to favour an EMI-aware design of the rotating machine at early stages when a physical prototype is not yet available. The developed modelling method is implemented and validated for two different PMSMs utilized in the automotive industry. These two machines are selected taking into account the INTERACT project boundaries and partners. In addition, the dissertation presents several experimental investigations aimed to further understand the contribution of the different machine constructive parts to the high-frequency impedance. Finally, a thorough sensitivity analysis is presented to exemplify the model applicability and to identify critical design parameters.

Two different PMSMs in the frame of INTERACT are utilized as a case study to implement the method. The applications of the two studied machines are a power steering (e-PS) and an Air Conditioning Compressor (ACC) unit (e-ACC) respectively. Both machines are three-phase PMSMs with concentrated winding and double-layer slots. One of them is a 0.5 kW, 10/12 machine with 8 turns per coil and the second machine is a 4kW, 8/12 machine with 28 turns per coil. ***Error! Reference source not found.*** summarizes the main characteristics and *Fig. 1* shows the cross-section for both machines.

Table I - Machines under study characteristics

	Machine 1 (e-PS)	*Machine 2 (e-ACC)*
Number of slots	12	12
Number of poles	10	8
Nominal power (kW)	0.5	4.7
Base speed (rpm)	1000	6000
Magnet remanence (T)	1.345	1.345
Turns/coil	8	28

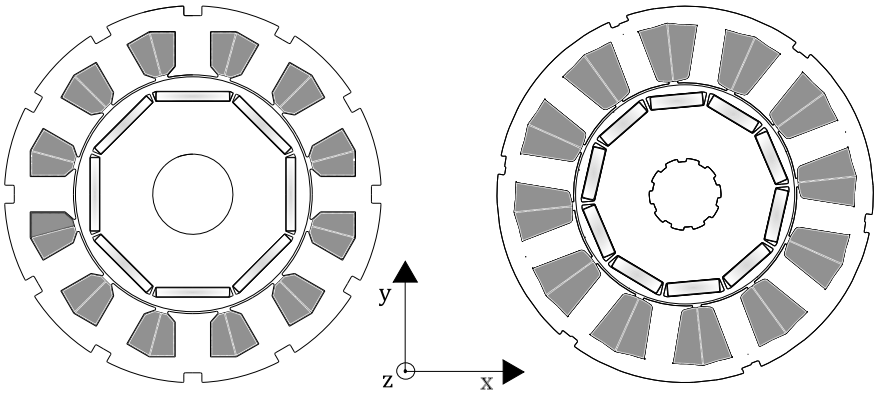

Fig. 1 - PMSMs under study cross-sections, (a) 8/10 e-ACC, (b) 10/12 e-PS

(a) (b)

The modelling method is built according to the following steps. First the equivalent circuit topology is selected based on multi-conductor transmission line theory. Then, the different machine parameters are extracted by using FEM. An electrostatic solver is utilized to obtain parasitic capacitances in the machine slots while frequency-dependent resistances and inductances are obtained by using a magnetodynamic solver. Once the parameters are obtained, they are integrated within the equivalent circuit following the frequency-dependent nature of resistances and inductances. Finally, DM and CM impedances over frequency are obtained by using a SPICE tool. *Fig. 2* shows a block diagram describing the proposed modelling method.

The type of equivalent circuit is decided based on multi-transmission line theory. the lumped equivalent circuit is considered the best option for the presented modelling method since it provides a good compromise between accuracy and computational cost. In addition, a pi-equivalent topology is chosen over the T-equivalent since frequency dependent parameters such as inductance and resistance are modelled just once. Each conductor in the machine slots is represented by a pi-equivalent section since they all have different parameters.

The parasitic capacitances are obtained by utilizing an electrostatic FEM solver. The

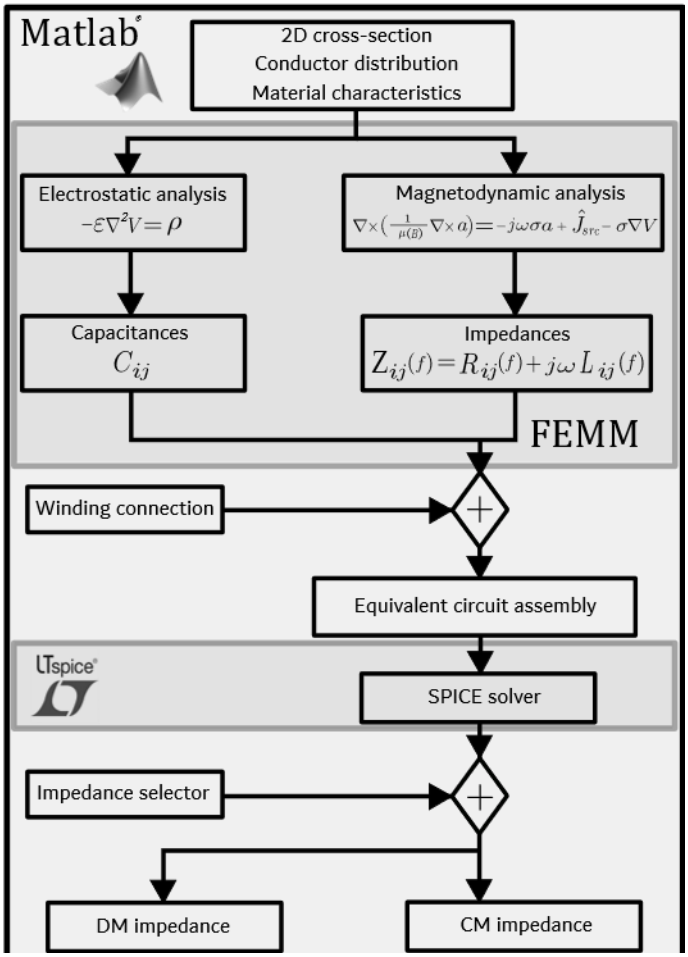

Fig. 2 - Modelling method block diagram

governing equation of such solver is given by:

$$-\varepsilon\nabla^2 V = \rho \quad \textbf{(0-1)}$$

where ε is the permittivity of the homogeneous region, V is the electric potential and ρ is the charge density. The different parasitic capacitances within the slot are organized in matrices. In this way, for each slot with a particular conductor distribution, a *NxN* matrix is obtained, where N represents the number of conductors in the slot. Each entry of the matrix is computed by setting the *i-th* conductor with a unitary voltage while the remaining *j-th* conductors and the slot walls are set to zero voltage. In this way, one analysis per conductor is carried out with each of the *i-th* conductors under 1V excitation. The surface charge on the *j-th* conductors and the iron walls represent the capacitance according to equation:

$$C = \frac{q}{V}\,[\mathrm{F}] \tag{0-2}$$

where q is the surface charge density of the conductors. *Fig. 3* illustrates the capacitance estimation method. The capacitance matrices for the e-ACC machine is presented in Fig. 4 .

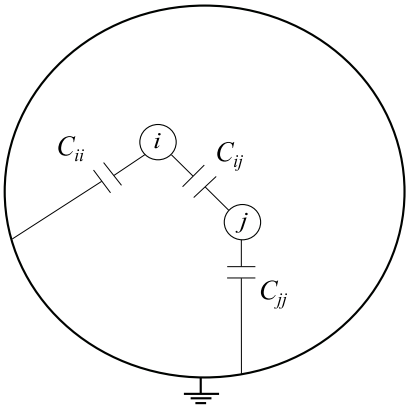

Fig. 3 - Capacitance extraction schematic

Frequency-dependent resistances and inductances are estimated by utilizing amgnetodynamic solver. The governing equation of such solver is given by:

$$\nabla \times \left(\frac{1}{\mu(B)} \nabla \times A\right) = -\sigma \dot{A} + \dot{J}_{src} - \sigma \nabla V \tag{0-3}$$

with A the complex magnetic vector potential, σ is the electrical conductivity, J_{src} the phasor transform of the applied source current, B the flux density and μ the magnetic permeability. The problem is solved in the frequency domain, where all AC quantities and A are expressed in phasorial notation.

The main challenge of the 2D FEM analysis is related to the flux penetration in the iron core. At high enough frequencies, eddy currents will start flowing within single lamination. These will create an increased reaction field that will confine the main magnetic field within the slot boundaries. Thus, at high-frequency excitations each single lamination in the iron core must be modelled to accurately map the inductance and resistance of each conductor. This is not a feasible implementation in practice since it would require a computationally expensive 3D simulation with a very fine mesh. To overcome this limitation and to enable the utilization of a coarse 2D mesh in the iron core, a homogenized iron core simplified model is built.

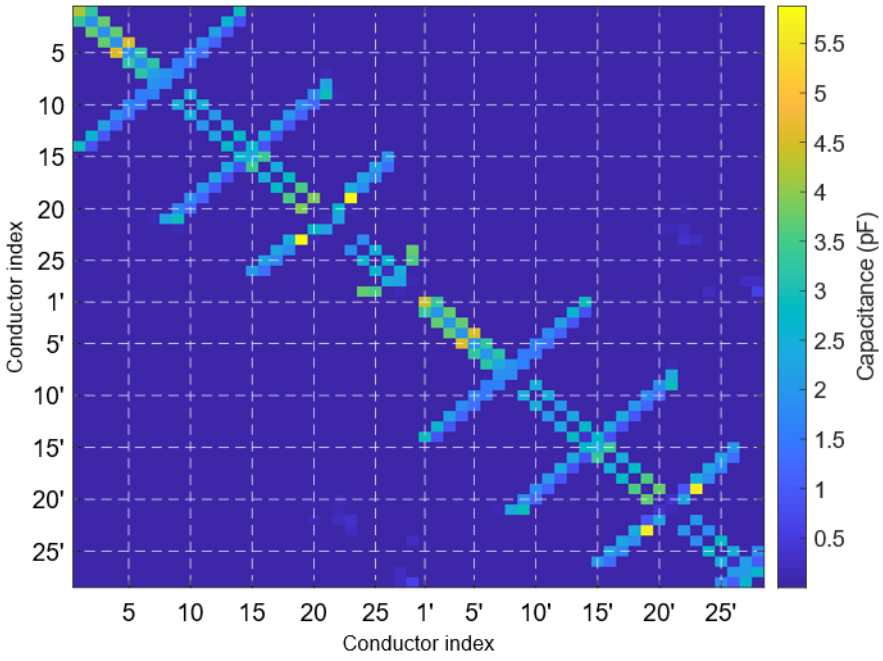

Fig. 4 - Example of capacitance matrix

The frequency dependent impedances for each conductor in the slot are computed by separately exciting each single conductor with a real-valued unitary current. The voltage drop on the excited conductor is the self-impedance and the voltage drops on the other slot conductors are the mutual impedances. Mutual effects between conductors of different slots are not considered since the flux penetration depth at high frequencies is smaller than the tooth width. The real part of the frequency-dependent impedances represents the resistive term (R), and the imaginary part is the reactance (X), from which the inductance value can be extracted by using the reactance definition ($X=j\omega L$). Thus, the real and imaginary terms of the machine impedances can be organized in matrices, where the diagonal entries represent the self-terms, and the off-diagonal entries represent the mutual couplings between conductors. *Fig. 5* shows the matrix representation for the resistances and the inductances of the e-ACC machine slot for different frequencies of excitation.

The frequency dependency of resistances and inductances is taken into account by using the Laplace transform together with active SPICE elements such as behavioral current and voltage sources. The utilization of pi-equivalent circuits makes possible to implement a single series impedance per-conductor, which eases the circuit implementation. The SPICE elements utilized in the circuit allow the usage of analytical expressions containing the Laplace variable (s). According to the definition of this variable, the frequency dependency can be easily described by using:

$$s = j\omega \xrightarrow{yields} f = \frac{s}{j2\pi} \qquad \textbf{(0-4)}$$

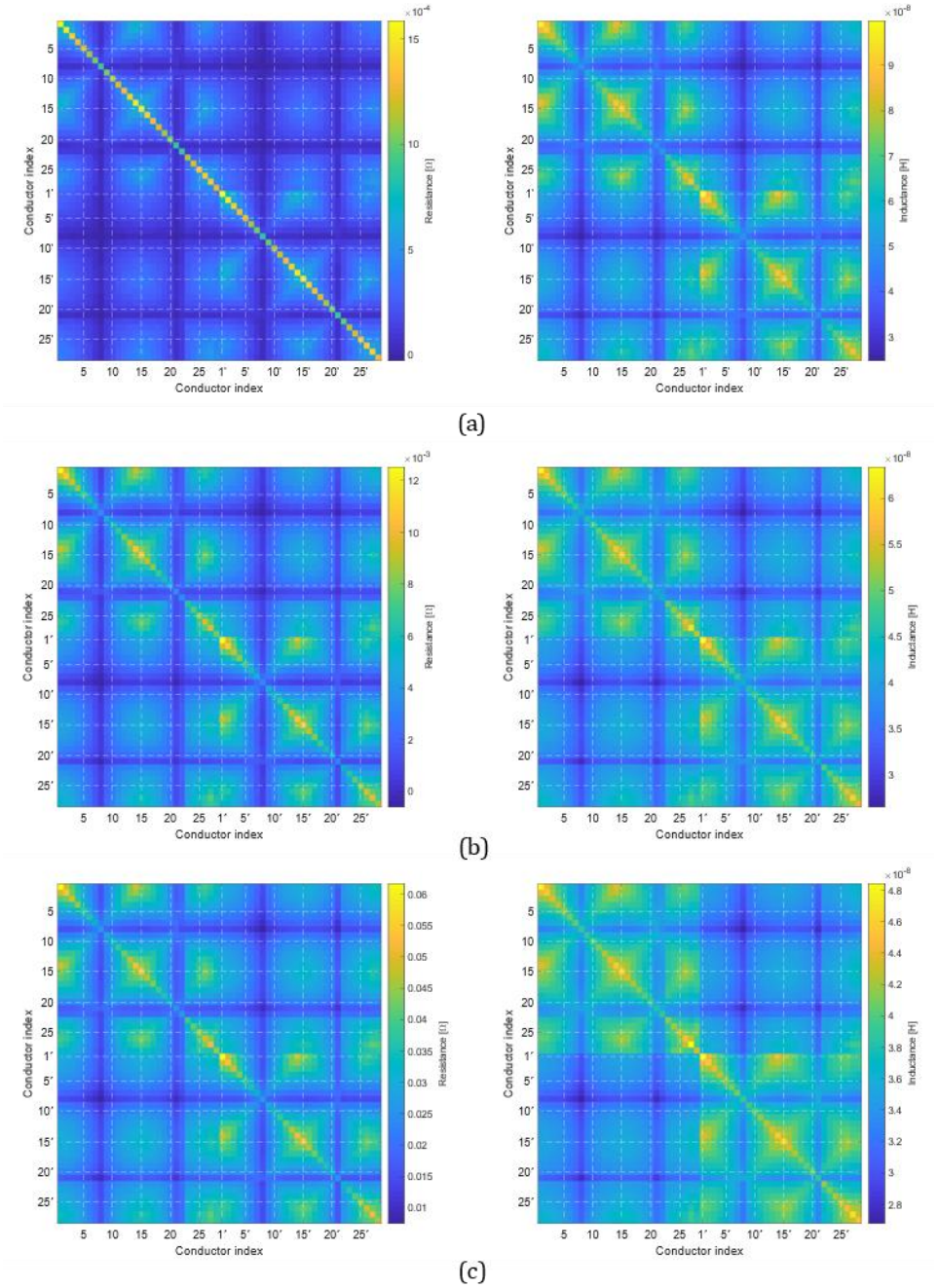

Fig. 5 - Impedance matrices for a slot with resistance (left) and inductance (right) terms, (a) 10 kHz, (b) 100 kHz, (c) 1 MHz

The last step for the frequency dependency implementation is to embed the impedance values for each conductor in the Laplace active sources. By combining equations (3-35), (3-36), and (3-38), the expressions for the impedance utilizing Laplace transform and power formulation are obtained:

$$\begin{cases} Z(s) = R(s) + jX(s) \\ R(s) = a_1 \left(\frac{s}{j2\pi}\right)^{b_1} + c_1 \\ X(s) = a_2 \left(\frac{s}{j2\pi}\right)^{b_2} + c_2 \end{cases} \quad \textbf{(0-5)}$$

These formulae are implemented in the active sources. *Fig. 6* shows the comparison between the impedances obtained from the active sources and the FEM simulations.

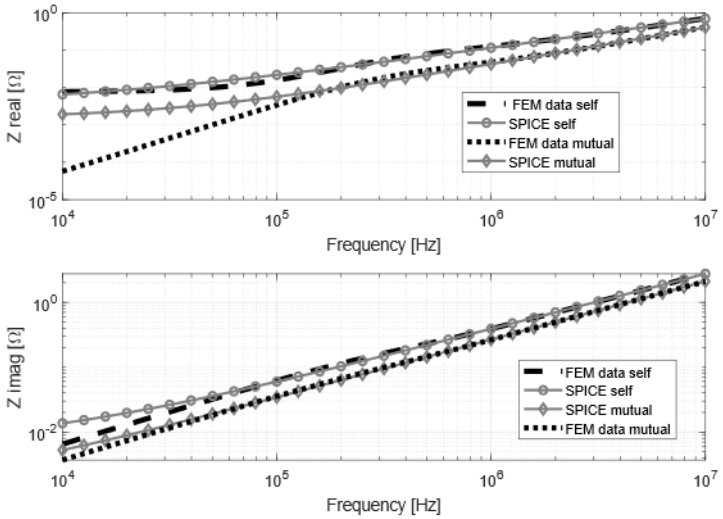

Fig. 6 - FEM vs SPICE self- and mutual impedances comparison

The frequency limits for the results simulations are set between 10 kHz and 30 MHz, with the upper limit corresponding to the CEs test upper frequency. The two modal impedances are obtained by injecting a real valued unitary current in the circuit according to two different connections. The voltage on the connection node is measured, which corresponds to the impedance. The DM circuit connection is made by connecting two different phases., while for the CM impedance the connection is made between the machine housing and the three phases in short-circuit. *Fig. 7* shows the schematic to obtain the two modal impedances. The simulation results for both case study machines and for both propagation modes are shown in *Fig. 8*. The impedance curves clearly differentiate both machines, where higher resonant amplitudes are obtained for the e-PS machine. The amplitude of the DM impedances over their inductive band presents a large variation, where the e-ACC shows higher values up to the resonant point.

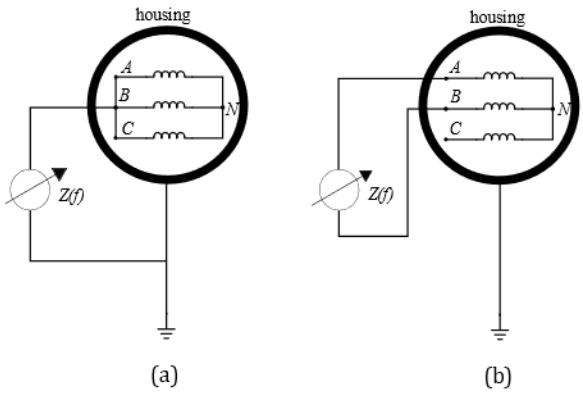

Fig. 7 - CM and DM connections for impedance computation, (a) CM, (b) DM

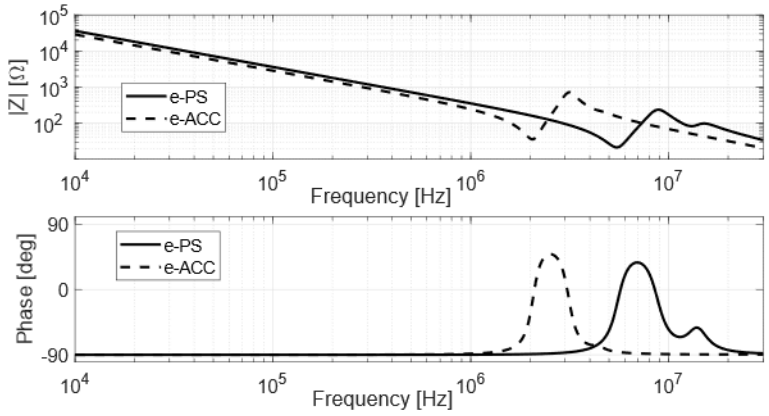

(a)

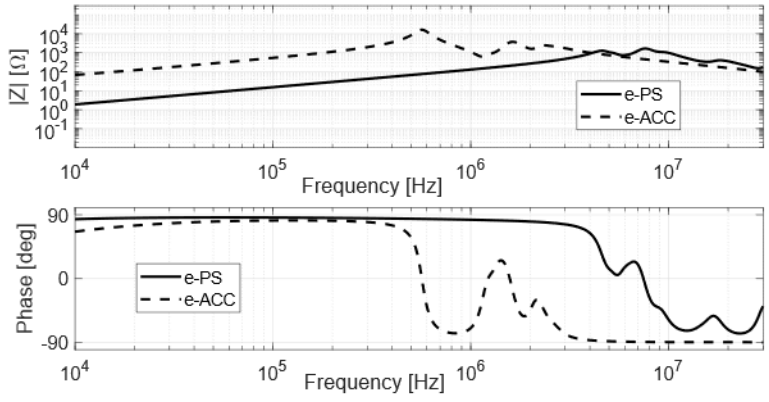

(b)

Fig. 8 - Simulation results, impedance absolute value and phase over frequency in the 10 kHz-30MHz range, (a) CM, (b) DM

The frequency range represents the most important parameter to choose the most feasible measuring method. In this dissertation, the focus is placed around the CEs frequency band including lower frequencies corresponding to typical switching frequency values (e.g., tenths of kHz). A precision impedance analyzer (Agilent 4294A) utilizing an auto-balancing bridge method represents the best option for accurate impedance measurement for the frequency range of interest. This equipment covers the frequency spectrum ranging from 40 Hz until 110 MHz.

The full machine impedance measurement including housing and rotor are utilized for validation. The rotor position and the phase combination are chosen arbitratily. The maximum frequency for validation is set at 30 MHz since the measurement accuracy starts to decrease from that frequency point on. Both machines were tested by utilizing an impedance analyzer (Agilent4294A), and the same test fixture and auxiliary cabling. The tests were performed in the same laboratory and by using the same impedance analyzer settings for both machines. Fig. 4 29 and Fig. 4 30 show the result comparison for the e-ACC and e-PS machine respectively.

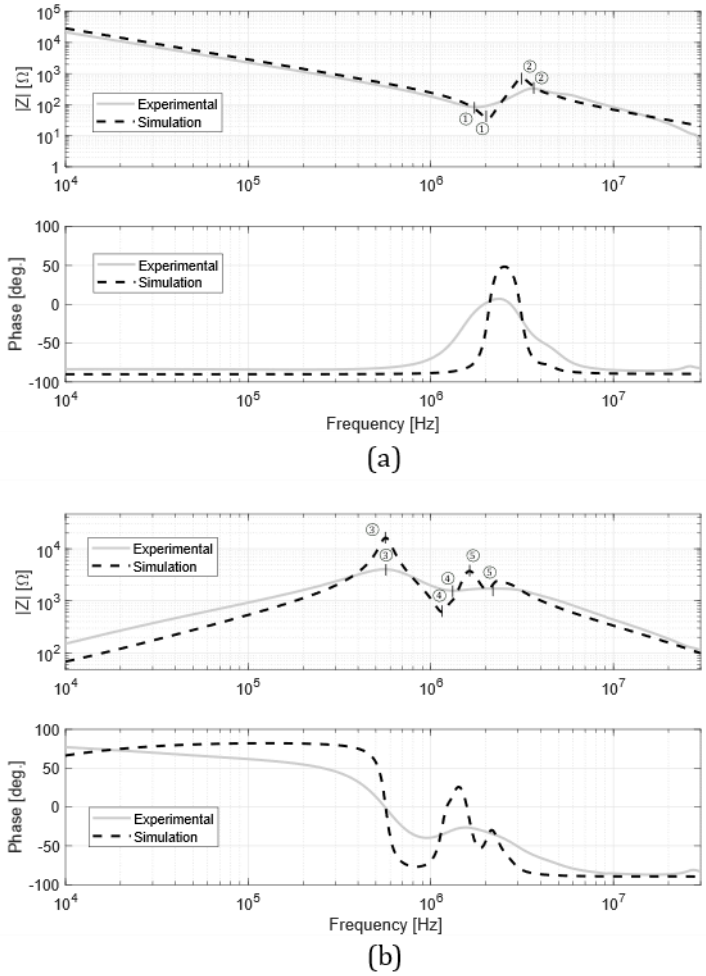

Fig. 9 - e-ACC machine experimental vs. simulation results, (a) CM, (b) DM

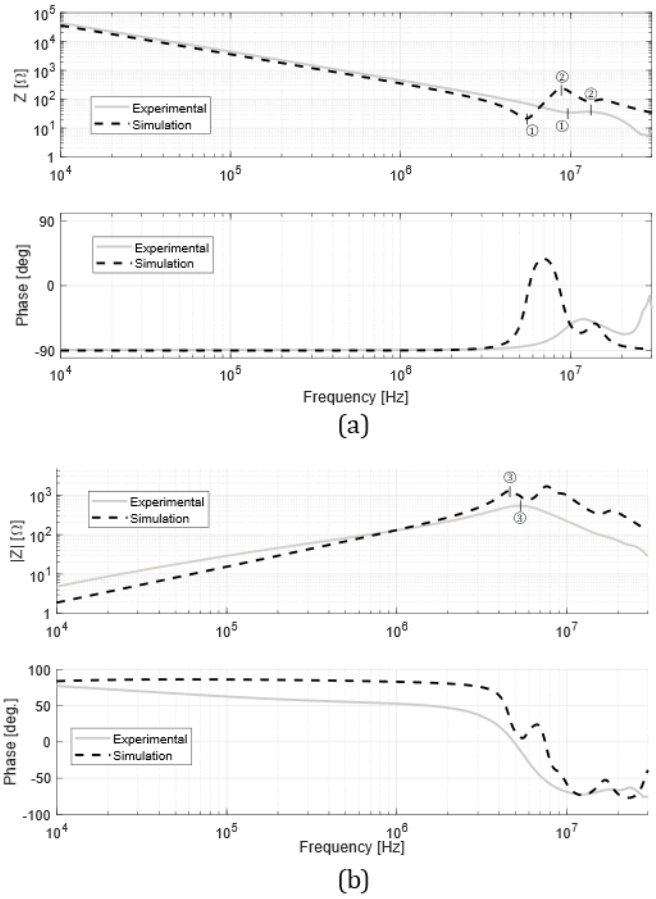

Fig. 10 - e-PS machine experimental vs. simulation results, (a) CM, (b) DM

The first conclusion that can be drafted from the comparison is that the simulated impedances match the general trend for both machines and both modes. This can be justified by the number of resonant points, and the inductive and capacitive behaviour over the different frequency bands. Another inmediate observation is the simulation lack of damping in the resonant points, which means that the resonances are sharper in the simulation than for the experimental measurements. In addition, some amplitude differences in the lower frequency bands (i.e., before the resonant points) can be easily observed for both machines and modes. These differences are more obvious in the DM than in the CM. In addition, the resonant points in the DM curves are closely matched while for the CM a disagreement is observed. The disparity is better observed in the e-PS CM curve. The antiresonance point in the e-PS machine DM curve is highly damped and not visible in the experimental results.

In spite of the evident inaccuracies, the presented modelling method manages to map the impedance response trends and their resonant points. In addition, by observing the impedance differences between the two different machines, the simulation results allow to distinguish between the two machines by just observing the impedance results. Thus, it is possible to state that the developed method can predict qualitative trends of the high-frequency impedance response in both propagation modes by utilizing a 2D machine cross-section, the conductor distribution within the slot, the winding connection scheme, and simple material characteristics.

A thorough sensitivity analysis is performed to check critical design parameters and to quantify model uncertainties. Several modelling levels are considered in the analysis. First, the direct impact of the primary parameters (RLC) is presented. Then, the winding connection effect is analyzed by utilizing a simplified model that allows to study the effect of series and parallel coil connection. In third place, the influence of the geometric parameters is studied. Finally, the effect of the material characteristics is studied. To limit the extent of the analysis, the most influent characteristics are considered and only one case study machine is utilized.

Conlusions and findings

1. On the modelling of high-frequency phenomena for rotating electrical machines

Chapter 2 provides a thorough literature review of the available high-frequency phenomena modelling methods. According to the parametrization of the model two different modelling trends were identified: test-based and numerical. From an electrical machine manufacturer perspective, the parametrization of the model defines the earliness of the model applicability. Thus, the numerical parameter estimation represents the only available option when machine prototypes are not yet available. A trade-off between accuracy, computational cost and complexity of the input data frames the high-frequency modelling for early-stage prediction.

2. On the modelling of high-frequency phenomena for rotating electrical machines

Chapter 3 presents a novel modelling method for high-frequency impedance prediction. The experimental validation for two different PMSMs is provided in Chapter 4.

The presented modelling method is implemented and validated on two different PMSMs with concentrated winding and double layer slots. The usage of experimental tuning and computationally expensive 3D simulations is avoided to satisfy the design framework. The input data is kept as simple as possible, which consists of 2D machine cross-sections, material characteristics provided by the motor manufacturer, stator winding connections, and the conductor distribution within the slot. Single slot conductors are modelled to consider inter-turn couplings. In addition, several complex high-frequency physical phenomena are considered in the method:

- Skin and proximitty effects are considered by adjusting the mesh thickness for each single conductor and for each simulation frequency

- Eddy currents flowing within single laminations at high frequencies are accounted by utilizing a homogenized iron core model. This is achieved by estimating a complex frequency-dependent relative permeability, which is modified for each simulation frequecy. Aditionally, the utilization of such homogenization technique allows the usage of a coarse mesh in the iron core, significantly reducing the computational cost.

- Iron core material characteristics at high frequencies are included in the homogenized iron core model. The only parameter extracted from the material data sheet is the low frequency relative pemeability (μ_(r,DC)), which is obtained from the BH curve at 50 Hz provided by the manufacturer.

- Frequency dependency of inductances and resistances is implemented in the circuit by utilizing Laplace expressions embedded into active circuit elements in the SPICE simulator. The usage of such expressions is limited to the frequency domain.

The dielectric losses in insulation elements cannot be estimated by utilizing a FEM solver. These have been considered in previous works by using experimental tuning, where the conductance of the turns is measured by using an impedance analyzer [83]. End-winding sections are not modelled to avoid three undesired scenarios. The first one is related to computationally expensive 3D simulations, since this is the common approach to model the end-winding electric and magnetic fields distribution [83], [93],[99]. The second obstacle is linked to the equivalent circuit computational efficiency, since end-winding sections add extra nodes to the linear system of equations to be solved in the SPICE solver. In third place, the end-winding geometry is seldom known with precision in early design stages. The method does not consider randomly wound machines, where the position of the conductors within the slot is not certainly known. However, the available slot area for conductor location is defined by geometric inputs such as fill factor, distance from simetry axis to last conductor, etc. The randomness of the conductor location is not assessed in the developed method.

The method is not intended to only achieve fast computational times but to satisfy the trade-off between accuracy, data simplicity and the simulation computational effort. The simulations are run from a Matlab general script, which calls, launches and retrieves results from the FEM and SPICE software. The device used for simulation is a Dell Precision 7520 with Intel(R) Core (TM) i7-7920HQ CPU (3.10GHz) and 31.19 Gb of usable RAM memory. A total of 12 frequency points between 10kHz and 10 MHZ are simulated for the magnetodynamic FEM analysis, while for the SPICE circuit 100 frequency points per decade are considered. The simulation times when simulating the e-ACC machine are shown in TABLE 6 I. The magnetodynamic FEM analysis represents a bottleneck for computation speed optimization.

Simulation part	Time
Electrostatic FEM	5 min 60 sec
Magnetodynamic FEM	4 h 38 min 40 sec
SPICE solver	3 min 55 sec

Regarding accuracy, the method shows large discrepancies in the amplitude for both machines and both modes. A clear lack of damping in the resonant points is observed, where the amplitude of the simulation clearly overcomes the measured one. However, resonant points, and phase and amplitude trends are properly maped. In addition, the two analyzed machines can be differentiated by analyzing their simulation results, where resonant peaks and amplitudes concomitant with each machine can be identified. The possible reasons for modelling inaccuracies are stated below:

- The lack of damping is motivated by the neglected resistive loses such as dielectric loses and small eddy current losses in the laminations. In addition,

small errors on the joule losses in the conductors, whch are properly taken into account, may be present.

- The neglected end-winding sections add extra overall resistance, reactance and capacitance. Even for a concentrated winding, (i.e. with short end-winding lenght) the effect of such parameters can affect the accuracy of the prediction.

- Inaccuracies in the material characteristics also affect the prediction. The material data is obtained from data sheet values.

- Inaccuracies derived from the motor manufacturing process and advanced development. Some examples can be a conductor missplacement, slot wall insulation irregularities, tolerances, stator welding, etc.

3. On the effect of housing and rotor in the high-frequency PMSM response

Chapter 4 fully describes the experimental measurement campaign. Within this chapter, the effect of rotor and housing insertion is experimentally assessed to increase the validation certainty. In addition, the effect of the rotor position is studied experimentally to analyze the influence of the DC magnetic field originated in the rotor magnets. In Chapter 5 the effect of the variation of the different RLC parameters and the numerical study of the rotor DC field effect are provided.

The housing insertion causes the amplitude to decrease in the CM impedance curve. In addition, the resonances of both CM and DM curve are slightly shifted towards lower frequency locations. These two variations indicate that the capacitance towards ground increases with the housing insertion according to the sensitivity analysis from Fig. 5 1. The DM impedance curve shows a light difference in amplitude all over its inductive part for the sample with housing and without rotor. The origin of this effect is uncertain since the inductive DM amplitude coincides for the stator sample and the full machine with housing and rotor.

The effect of the rotor insertion cannot be fully evaluated from Fig. 4 20 since the rotor position is, a priori, not known. The experimental study of the rotor position is presented in detail in Fig. 4 22,Fig. 4 24, Fig. 4 23. The rotor position mainly affects the inductive amplitude of the DM curves for the different phase combinations. This increase indicates that the reactance of the coils is affected by the saturation in the iron (see Fig. 5 4). From the study presented in section 4.6, it is demonstrated that the highest DM amplitudes are obtained for rotor positions where the averaged B-field in the coils of the connected phases is low valued (see TABLE 4 II, and TABLE 4 III). The DM amplitude variation concords with the numerical study presented in section 5.4.2, where the magnet remanence effect on the impedance response is evaluated. The analysis points out that for reduced averaged B-field in the coils, the reactance of single conductors slightly increases. Therefore, the DM amplitude over their inductive band increases as well. However, the variation of the low-frequency relative permeability depending on the averaged B-field, does not have a significant effect in the numerically predicted impedance response as shown in Fig. 5 19. The contribution of the housing and rotor to the high-frequency impedance response of a PMSM can be summarized as follows:

- The housing inserts additional turn-to-ground capacitance, slightly lowering the amplitude in the CM response and slightly shifting the resonant points towards lower frequencies.
- The rotor contribution can be deduced from the DM amplitude over its inductive band (i.e. in this case from 10 kHz to approx. 600 kHz). The rotor position defines the B-field in the iron of the stator coils, which influences the instantaneous working point in the hysteresis charcteristic. Thus, for reduced average B-field in the connected phases, the amplitude of the DM impedance slightly increases. This is supported by the numerical computation of the low-frequency relative permability. However, the utilized numerical model does not properly map this effect since low-frequency relative permeability variation does not significantly affect the impedance curves, while the amplitude difference is obvious for the experimental test.

- The stator winding represents the main contribution to the high-frequency impedance response for both propagation modes. The insertion of the housing and the rotor do not represent a critical variation of the impedance trends and resonant point location.

4. Identification of critical design parameters and quatification of model uncertainties

Chapter 5 presents a detailed sensitivity analysis separately studying the effect of the RLC parameters, geometric parameters, stator winding connection, and material properties in the high-frequency impedance response.

The effect of the RLC parameter variation is used as a reference to evaluate possible model inaccuracies and improvements. The connection of the different coils (i.e., series or parallel connection) heavily affects the impedance. It has been demonstrated that the series connection of coils varies both the amplitude of the impedances and the location of resonant points. For parallel connected coils, the resonances are kept at a fixed frequency, while the amplitude is directly affected.

The shape of the slot will directly affect all the parameters of the equivalent circuit. This feature is not studied because it represents the base input for the model. The impact of the stack length, conductor diameter, slot wall insulation thickness and turns-per-coil is studied. The stack length and the number of turns-per-coil represent the most critical parameter affecting the high-frequency impedance response. A lower impact is observed for the variation of the conductor diameter, while slot wall insulation thickness slightly affects the CM impedance curve, showing a neglegible influence on the DM response.

The most critical material characteristic affecting both impedance curves is the slot wall insulation permittivity, which clearly affects capacitive amplitudes and the location of the resonant points. Copper conductor conductivity does not affect significatively the impedance for values around the range of tenths of MS/m. The magnet remanence and the type of electrical steel affect the estimated low-frequency relative permeability value. The variation affects the effective permeability over the lower frequency band. However, the alteration of such parameter does not significatively affect the impedance curves.

The presented sensitivity analysis identifies several basic critical design parameters affecting the high-frequency impedance response. These are numbered as follows:

- Stator winding connection
- Stack length
- Number of turns-per-coil
- Conductor diameter
- Slot wall insulation permittivity

The numerical estimation of the high-frequency impedance response in rotating electrical machines presents a large number of challenges to be addressed in future research works.

The presented method should be tested in machines without DC field in the rotor such as induction and pure synchronous reluctance machines. The validation for stators with distributed winding should be also performed since they present larger end-winding sections, which may reduce the accuracy of the method. The sensitivity analysis of the design parameters can be addressed from an experimental perspective by building custom machine stator samples with different stack length, turns-per-coil, conductor diameter, etc.

The accuracy of the method can be enhanced trough the development of a reduced 2D end-winding model accurately mapping parasitic capacitances and frequency-dependent RL parameters. The FEM estimation of RLC parameters in coils surrounded by laminated iron cores can be further validated by studying simple coils. The estimation of dielectric losses in the insulation elements without utilizing experimental tuning would also represent an accuracy improvement since the damping in the resonant points would significatively increase. The computation speed could be optimized by further simplifying the estimation of RL parameters in the magnetodynamic FEM solver.

The method shows potential applicability for stator fault prediction since the winding connection affects the impedance response of the machine in both modes. The modelling approach could help on predicting the impedance changes when a short circuit within the winding occurs. Finally, the measurement of the machine impedance on-line instead of in standstill conditions could represent an advantage for the numerical prediction of EMI and for the method applicability in the condition monitoring and fault diagnosis field.